Performance and Optimization of Outage Probability in CBTC Systems

Do Viet Ha[1], Tu Lam Thanh[2], Trinh Thi Huong[1], and Trinh Van Chien[3]
[1] University of Transport and Communications, Hanoi, Vietnam
[2] University of Poitiers, Poitiers, France
[3] University of Luxembourg, Luxembourg
Email: dovietha@utc.edu.vn; {lamthanh0; trinhchien.dt3}@gmail.com; trinhhuong@utc.edu.vn

***Abstract*—The performance of two access points (APs) Communication-Based Train-Control (CBTC) systems subjected to an imperfect Channel State Information (CSI) scenario is investigated. More precisely, we first model the realistic small-scale fading distribution for which the receiver only has the outdated CSI due to the mobility of the train. We then derive the Outage Probability (OP) of the train and the ergodic capacity of the system in the closed-form expression based on the considered channel model. Additionally, we formulate an optimization problem that minimizes the maximal OP, which corresponds to the location of the train. For such, the Signal-to-Noise-Ratio (SNR) is minimized as a function of the position of two APs. The pattern search method is utilized to solve the considered minimization problem. Numerical results confirm that by the optimal placement of the position of APs, the OP can be significantly ameliorated compared to the other placement methods. Furthermore, the numerical results also illustrate that the proposed solution completely coincides with the exhaustive search but with much less computation time. Finally, the mathematical framework is verified extensively by Monte Carlo simulations.**

***Index Terms*—Outage probability, CBTC, optimal placement, Monte-Carlo simulations, Imperfect CSI.**

I. INTRODUCTION

Metro systems are considered the most efficient transportations in metropolises thanks to their good system throughput, high reliability, and environments friendly. However, the ever-increasing population in these mega-cities has posed higher demands and standards for example, safer and higher efficiency. Recently, the rapid development of wireless technologies such as 5G [1] and low power wide area networks (LPWAN) (Sigfox, long-range (LoRa) [2]) has regarded as a cost-effective and high-efficiency solution to satisfy these requirements. To be more specific, a Communication-Based Train Control (CBTC) system empowered by wireless communications is an automatic train signaling system that guarantees safe and swift communications between trains and ground stations [3]. In CBTC systems, ensuring high reliability and continuous interconnection between trains and zone controller subsystem (ZC) is the backbone of the whole system. Nevertheless, like all wireless communications networks, the performance of a CBTC system completely relies on the Signal-to-Noise-Ratio (SNR) at the receiver which is a composite function of several uncertainty factors such as the fading channels, the large-scale path-loss, the shadowing and the transmit power and so on [4], [5]. There are many doable solutions to boost up the SNR such as installing more Access Points (AP), turning up the transmit power, and optimizing the location of APs, and so forth. Among these solutions, the optimal placement of APs is regarded as the most cost-effective and high-efficient one since it does not require either to install more APs and/or increase the transmit power thus reducing both the capital expenditure (CAPEX), and the operating expenditure (OPEX). As a result, in the present paper, we first address the performance of the CBTC systems via two popular metrics, the Outage Probability (OP) and the ergodic capacity. We then minimize the OP by optimally placing the position of the APs. In the following section, we first study the state-of-the-art of CBTC systems before going to highlight our novelties and contributions.

The performance of the CBTC system was studied extensively in the literature [6]-[14]. More precisely, the outage probability and the Bit Error Rate (BER) of the cooperative relaying CBTC system were investigated in [6]. Additionally, this work also proposed an optimal guidance trajectory calculation scheme to mitigate the handoff latency in cooperative communications. However, this work does not focus on optimizing the position of the APs. To further enhance the performance of CBTC such as handoff latency, authors in [7] proposed to employ coordinated multipoint (CoMP) to simultaneously serve the train by many Base Stations (BSs). This work again focuses on minimizing the communication latency. The packet drops introduced by random transmission errors and handovers was examined in [8], where a group of train were studied together rather than a single train. Both the field test and computer-based simulations were presented, and the outcomes were far better than other schemes in terms of energy consumption and riding comfortability. This work, however, concentrates on minimizing energy consumption by reducing unnecessary traction and brake forces. The train-ground communica-

Manuscript received May 14, 2021; revised July 20, 2021; accepted July 30, 2021.
Corresponding author: Do Viet Ha (email: dovietha@utc.edu.vn).
This research is funded by University of Transport and Communications (UTC) under grant number T2020-DT-005TĐ.

doi: 10.18178/ijeetc.10.6.439-447

tions field test was conducted on the ring rail line of the Beijing transport system based on long term evolution (LTE) technology in [9]. The results reveal that LTE technology is feasible to deploy in CBTC communications along with the traditional Wireless Local Area Networks (WLAN). The work in [10] also employed LTE-M as the main wireless interface for train-ground communications. They proposed a new scheme called the FlashLinQ-based Train-to-Train communication scheme to enhance the reliability and latency of the CBTC systems. The quantified resilience is used as a principal metric to evaluate the preservation and recovery performance of CBTC systems. Q-learning is then to generate optimal control strategies considering all trains, ground parameters. Authors in [11] addressed the problem of energy-efficiency of train-ground communications by employing mmWave. More specifically, the paper proposed an energy-efficient power control scheme which considers a multi-lobe antenna and a position-prediction modelling to minimize the total power consumption. A MIMO-assisted handoff (MAHO) scheme was introduced in [12] to reduce the handoff latency in CBTC systems. During the handoff procedure, the train is able to communicate with both serving AP and the candidate AP thanks to multiple antennae where some are used to exchange the data and others are yield to transmit/receive the signaling information. The proposed scheme is superior to the conventional break-before-make scheme in terms of the frame error rate of the handoff signaling, the error-free period. A novel design of the Automatic Train Operation (ATO) subsystem was proposed in [13] that took into consideration the train load and delays in the line that were ignored by the conventional design. More precisely, the design comprises of two main steps. In the first step, an optimal Pareto front for ATO speed profiles is built which is changeable according to the train load. In the second step, from the robust Pareto front, a set of speed profiles are selected to be programmed in the ATO equipment. The results illustrated that the energy consumption can be saved between 3% and 14%. A cognitive control approach was applied to CBTC systems in [14] where the wireless channel is modelled by finite-state Markov chains and the channel state transition probability matrices were derived from the real field measurement. Reinforcement learning was utilized to obtain the optimal policy based on the performance measure that comprises of the information gap and the linear quadratic.

Nevertheless, these above works mainly address the minimization of the handoff latency, the reduction of energy consumption, the packet drops and the design of the ATO subsystem rather than optimizing the placement of the APs. Although the optimized placement of APs of a general wireless network were studied widely in the literature [15], [16], a few works investigate the performance of the CBTC system by optimally deploying the APs [17], [18]. Particularly, in [17] the authors optimized the placement of APs to minimize the path-loss from train to ground and vice versa. However, this work ignores the impact of fading which is critical in wireless communications. The authors in [18] relied on the exhaustive search to find out the optimal deployment of the APs.

Different from the above-mentioned works, in the present paper, the OP and the ergodic capacity of a two APs CBTC system is computed in the closed-form expression under the imperfect Channel State Information (CSI) scenario. Additionally, we minimize the worst OP by optimally locating the positions of APs. The main contributions and novelties of the paper are as follows: *i)* The outage probabilities and the ergodic capacity subjected to both small-scale fading and large-scale path-loss under imperfect CSI scenario are computed in the closed-form expression; *ii)* The minimization problem of the worst OP is formulated and figured out by the pattern search method; *iii)* The accuracy of the proposed framework is extensively verified by Monte-Carlo simulations.

The paper is organized as follows: In Section II, an overview and the impact of the imperfect CSI on the CBTC systems are discussed. Moreover, Section III provides the system model in detail. In Section IV, performance analysis and optimization of the outage probability are investigated. In Section V, Monte Carlo simulations are supplied to clarify the correctness of our framework. Finally, Section VI draws the main conclusions of this paper.

II. CBTC Systems

A. Overview of CBTC Systems

A CBTC system consists of four subsystems, namely, the train–ground communication subsystem, the zone controller (ZC) subsystem, the automatic train supervision (ATS) subsystem, and the vehicle onboard control subsystem as shown in Fig. 1. The vehicle onboard control subsystem makes up by two subsystems, i.e., the Automatic Train Protection (ATP) and automatic train operation subsystems (ATO).

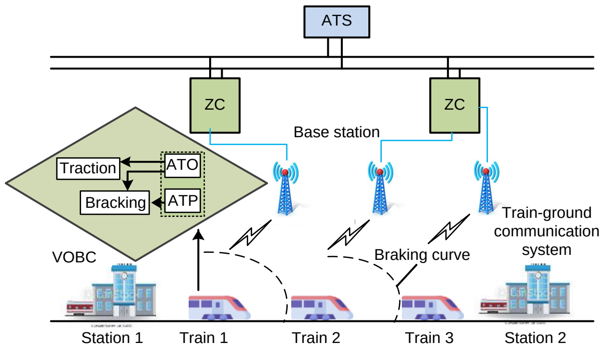

Fig. 1. A communication-based train-control system [8].

The ATS subsystem creates the scheduling for all trains and sets the trip time between two stations. The ATO subsystem will then find out an optimal guidance trajectory based on the trip time report of the ATS and other performance indexes such as the comfortable of the passengers and the energy consumption. The guidance trajectory is a velocity profile which provides the optimal velocity for each specific position. Concerning the ATO subsystem, its main function is to bring the train to operate at the given guidance trajectory. Different to the conventional fixed-block track circuit, in CBTC systems, the continuous communications between the train and APs are applied. To do it, the considered systems divide the railway into non-overlap sections where each section is controlled by a ZC center that employs its own wireless communications systems. The position, direction, identity and velocity of each train are then transmitted to the ZC via the APs installed at both sides of the railway. The communications between trains and the ZC via the APs must be continuous to allow the ZC to identify the location of all trains associated to its coverage area in a real-time manner. Having obtained the position of all trains as well as all obstacles along the railway, the ZC transmits a movement authority (MA) to all trains in its service area. It is noted that the MA of a train is the zone from end of the train to the obstacle in front of the train. The automatic train protection subsystem on the train will estimate the real-time braking curve based on the latest received MA. The ATP system will activate the emergency braking once the velocity reaching the target velocity on the service braking curve and this action is taken place prior to the ATO subsystem in order to protect the train go out of its MA and thus guaranteeing the safety of the train as well as the whole system.

B. Impact of the Imperfect CSI on the CBTC Systems.

It is obvious that under the perfect CSI, train will operate smoothly according to it real-time MA and it will never reach its target velocity on the braking curve despite of travelling on the same guidance trajectory with others train. However, under the impact of imperfect CSI, the train may not get the latest MA message from the coordinated ZC. Thus, there is high probability that train will use the outdated MA and its ATP subsystem will begin brake service to ensure the train not travelling out of its MA. Once the ATP subsystem has the updated MA, it will then stop the brake service, the ATO subsystem will re-control the train and bring it back to the original optimized guidance trajectory. It is noted that due to the outdated CSI, the train will possibly travel off its intended guidance trajectory. In the worst case, the ATP subsystem will stop the train in case the delay of MA is too long. As a result, it will consume much energy and reduce the comfortable of passengers. Additionally, the trip time between stations will be turned up and will affect the other trains operation. The ATS subsystem will also need to modify its timetable and enhance the departure time interval of each train that is significantly scaling down the efficiency of the railway utilization. Hence, it is important to investigate the impact of the imperfect CSI in the CBTC systems.

III. System Model

A. Networking Modelling

We consider a train-ground communications system comprising two APs, which situate along the two-side of the track and a train running on the track as shown in Fig. 2 (The system-level performance under a multiple APs and trains system is left for future work). In CBTC systems, wireless communications are employed to communicate between trains and APs. Particularly, an antenna is mounted on the top of the train to either transmit or receive information from the system via the APs. Let us denote $\mathbf{X}_1 = (x_1, h_1), \mathbf{X}_2 = (x_2, h_2)$ and $\mathbf{T} = (z, h_{\text{tr}})$ are the vector that contains the horizontal and altitude values of AP1, AP2 and the train. More precisely, $x_1, x_2, z \in [0, D]$ are the horizontal coordination of the APs and the train while $h_1, h_2 \in \left[h_{\min}^{\text{AP}}, h_{\max}^{\text{AP}}\right]$ and h_{tr} are the attitude of the antenna of the APs and the train. The symbol D is the length of the considered track; $h_{\min}^{\text{AP}}$ and $h_{\max}^{\text{AP}}$ are the minimum and maximum height of the APs. In the present work, we assume that the attitude of the train's antenna is fixed as a typical assumption in the reality.

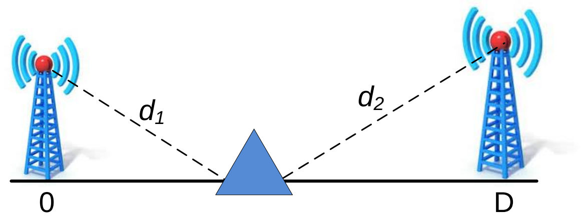

Fig. 2. The considered simplified train-ground communications in a CBTC systems.

B. Channel Modelling

1) Small-scale fading

All transmission links are subjected to Rayleigh fading. It is noted that Rayleigh fading is considered due to its severe performance. Thus, it is regarded as the lower bound of other fading such as Rician, Nakagami-*m* and composite fading. In Section V, numerical results are provided to verify this trend. The mathematical framework under these distributions, however, is left for future work. Additionally, we consider the imperfection of channel coefficient due to the mobility of the train. Particularly, the relation between the actual channel coefficient denoted by g and its estimated version denoted by χ is formulated as follows [19]:

$$\chi = \rho g + w\sqrt{1-\rho^2}\,, \tag{1}$$

where $\rho = J_0^2\left(2\pi f_d T_b\right) \in [0,1]$ is the correlation efficiency between the actual and estimated version; $f_d = v f_c / c$ is the maximal Doppler frequency; f_c, c are the carrier frequency (in Hz) and the speed of light (in meter per second); v is the velocity of the train (in meter per second); T_b is the interval sampling time (in second); $J_0(\cdot)$ is the zero-order Bessel function of the first kind [20]; $\sqrt{\cdot}$ is the square root function and w is the complex Gaussian random variable (RV) with variance σ_g^2 and is independent of g.

2) Large-scale path-loss

Let us denote $d_u, u \in \{1,2\}$ as the Euclidean distance between the train and the AP$_u$, the large-scale path-loss is given by [21]:

$$L_u = K_0 d_u^\eta,\ u \in \{1,2\}$$
$$d_u^\eta = \left(\sqrt{(z-x_u)^2 + (h_{\text{tr}} - h_u)^2}\right)^\eta, \tag{2}$$

where $K_0 = (4\pi f_c/c)^2$, $\eta > 2$ are the path-loss constant and the path-loss exponent, respectively.

3) Signal-to-noise ratio (SNR)

In the considered CBTC system, the train is served by the AP which has the larger signal-to-noise ratio at the train. Mathematical speaking, the end-to-end SNR at the receiver is formulated as [22]:

$$\text{SNR}_{\text{e2e}} = \max\{\text{SNR}_1, \text{SNR}_2\}$$
$$\text{SNR}_1 = \frac{\rho^2 P_1}{\sigma^2 L_1}|g_1|^2, \quad \text{SNR}_2 = \frac{\rho^2 P_2}{\sigma^2 L_2}|g_2|^2, \tag{3}$$

where P_1 and P_2 are the transmit power of AP1 and AP2; $\sigma^2 = \sigma_g^2(1-\rho^2) + \sigma_r^2$ is the noise variance at the train; $\sigma_r^2 = -174 + \text{NF} + 10\log_{10}(\text{BW})$ (dBm) is the noise variance of AWGN noise at the train; NF is the noise figure at the receiver; BW is the transmission bandwidth; and $|g_u|^2, u \in \{1,2\}$ is the channel gain from AP$_u$ to the train.

IV. Performance Analysis and Optimization

A. Performance Analysis of Outage Probability (OP)

The OP is the probability that the signal-to-noise ratio at the train is below the pre-defined threshold and is formulated as follows [5]:

$$\text{OP}(\tau) = \Pr\{\gamma = \text{SNR}_{\text{e2e}} < \tau\} = F_\gamma(\tau) \tag{4}$$

Here $\tau = 2^{R/BW} - 1$ is the pre-defined threshold and R is the required achievable rate (in bit/s); $F_\gamma(\cdot)$ is the cumulative distribution function (CDF) of the random variable (RV) γ. In order to compute the OP in (4), the following lemma is useful and is given as

Lemma 1: Given N independent and non-identical distribution (i.n.i.d.) RVs with CDF $F_{Y_i}(y)$, the CDF of the maximum of N RVs are given as

$$F_Z(z) = \Pr\{Z = \max\{y_1, y_2, \cdots, y_N\} < z\} = \prod_{i=1}^{N} F_{Y_i}(z) \tag{5}$$

Proof: The proof is obtained straightforwardly by employing ([23]: Eq. 2.1.1). Q.E.D.

From Lemma 1, the OP in (4) is calculated as follows:

$$\text{OP}(\tau; \mathbf{T}, \mathbf{X}_1, \mathbf{X}_2) = \left(1 - \exp\left(-\frac{\tau\sigma^2 L_1(\mathbf{T}, \mathbf{X}_1)}{\rho^2 P_1 \Omega_1}\right)\right) \times \left(1 - \exp\left(-\frac{\tau\sigma^2 L_2(\mathbf{T}, \mathbf{X}_2)}{\rho^2 P_2 \Omega_2}\right)\right). \tag{6}$$

Equation (6) is obtained straightforwardly by employing Lemma 1 and the CDF of the exponential function. Q.E.D.

Remark: It should be noted that the OP in (6) is computed at a specific position of the train, not on the average or the maximum (the worst position).

In the next section, we are going to minimize the OP of the worst position in order to guarantee the quality-of-services (QoS) of the whole system.

B. Ergodic Capacity

In this section, the ergodic capacity measured in [bits/s/Hz] of the proposed system is computed as follows [24]:

$$\bar{C} = \frac{1}{\log(2)} \left[\begin{array}{l} I_1\left(\frac{\sigma^2 L_1(\mathbf{T}, \mathbf{X}_1)}{\rho^2 P_1 \Omega_1}\right) + I_1\left(\frac{\sigma^2 L_2(\mathbf{T}, \mathbf{X}_2)}{\rho^2 P_2 \Omega_2}\right) \\ -I_1\left(\frac{\sigma^2 L_1(\mathbf{T}, \mathbf{X}_1)}{\rho^2 P_1 \Omega_1} + \frac{\sigma^2 L_2(\mathbf{T}, \mathbf{X}_2)}{\rho^2 P_2 \Omega_2}\right) \end{array} \right], \tag{7}$$

where log(.) is the logarithm function; $I_1(x) = \exp(x) E_1(x)$, $E_1(\cdot)$ is the exponential integral function defined in [25].

Proof: The proof is provided as follows:

$$\begin{aligned} \bar{C} &= \text{E}_\gamma\{\log_2(1+\gamma)\} = \int_0^\infty \log_2(1+x) f_\gamma(x) dx \\ &\overset{(a)}{=} \frac{1}{\log(2)} \int_0^\infty \frac{\bar{F}_\gamma(x)}{1+x} dx = \frac{1}{\log(2)} \int_0^\infty \frac{dx}{1+x} \\ &\times \left(\begin{array}{l} \exp\left(-\frac{x\sigma^2 L_1(\mathbf{T}, \mathbf{X}_1)}{\rho^2 P_1 \Omega_1}\right) + \exp\left(-\frac{x\sigma^2 L_2(\mathbf{T}, \mathbf{X}_2)}{\rho^2 P_2 \Omega_2}\right) \\ -\exp\left(-\frac{x\sigma^2 L_1(\mathbf{T}, \mathbf{X}_1)}{\rho^2 P_1 \Omega_1} - \frac{x\sigma^2 L_2(\mathbf{T}, \mathbf{X}_2)}{\rho^2 P_2 \Omega_2}\right) \end{array} \right) \\ &\overset{(b)}{=} \frac{1}{\log(2)} \left[\begin{array}{l} I_1\left(\frac{\sigma^2 L_1(\mathbf{T}, \mathbf{X}_1)}{\rho^2 P_1 \Omega_1}\right) + I_1\left(\frac{\sigma^2 L_2(\mathbf{T}, \mathbf{X}_2)}{\rho^2 P_2 \Omega_2}\right) \\ -I_1\left(\frac{\sigma^2 L_1(\mathbf{T}, \mathbf{X}_1)}{\rho^2 P_1 \Omega_1} + \frac{\sigma^2 L_2(\mathbf{T}, \mathbf{X}_2)}{\rho^2 P_2 \Omega_2}\right) \end{array} \right], \end{aligned} \tag{8}$$

where $\text{E}\{\cdot\}$ is the expectation operator; $\bar{F}_X(x) = 1 - F_X(x)$ is the complementary CDF (CCDF) of the random variable X; (a) is held by utilizing integration by parts; (b) achieves with the help of [20, 3.354.4] and we close the proof here.

C. Optimisation Problem

The optimization problem is formulated as follows:

$$\begin{aligned} &\min_{\mathbf{X}_1, \mathbf{X}_2} \quad \max_{\mathbf{T}} \{\text{OP}(\tau; \mathbf{T}, \mathbf{X}_1, \mathbf{X}_2)\} \\ &\text{s.b.t} \quad x_1, x_2 \in [0, D],\ h_1, h_2 \in \left[h_{\min}^{\text{AP}}, h_{\max}^{\text{AP}}\right]. \end{aligned} \tag{9}$$

Examining (9), we observe that the considered problem is non-convex owing to the non-convex objective function. To find the optimal solution in (9), we employ the Hooke and Jeeves pattern search (or direct search) method [26]. The advantage of the pattern search method is gradient-free; it, as a result, is suitable for the discontinuous problem. There are two main steps in the Hooke and Jeeves algorithm, namely, the exploratory move and the pattern move. In the first step, i.e., the exploratory move, for each direction, the solver will locally examine the performance of the objective function by increase and decrease the coordinate of the base point denoted by $\mathbf{p}^{(0)}$ in that direction with step size ε, then choosing the coordinate which provides the best performance. Here $\mathbf{p}^{(i)}$ is the coordination vector at the step (i). The exploration steps continuous for all the directions and we temporarily obtain the next point denoted as $\mathbf{p}^{(1)}$. It is noted that the step size ε is not necessarily the same for all directions. In the second step, i.e., the pattern moves, after acquiring the information of all directions in the first step, the next point denoted by $\mathbf{p}^{(2)}$ is identified as $\mathbf{p}^{(2)}=\mathbf{p}^{(1)}+(\mathbf{p}^{(1)}-\mathbf{p}^{(0)})$. Although the direct search is based on heuristics, not on rigorous mathematical theory, a large number of studies have proven the convergence of pattern search methods [26], [27].

V. Numerical Results

In this section, we provide numerical results to confirm the accuracy of our mathematical framework in the previous section. Unless otherwise stated, the following parameters are yield in this section: $\Omega_1=\Omega_2=2$, D=500m, NF=6dB, BW=20MHz, f_c=2.4GHz, η=2.1, P_1=30dBm, P_2=40dBm, R=100kbits/s, v=60km/h, T_b=0.1ms, $\sigma_g^2=1$, $z=0:0.5:D$ m, $h_1,h_2\in[5,10]$ m, and $h_{tr}=3.8$ m.

Fig. 3 illustrates the outage probability versus the x-coordinate of the train under the fixed deployment of APs $\mathbf{X}_1$=(125,6), $\mathbf{X}_2$=(375,8) with different velocities, i.e., $v=30,60,90$ km/h. In Fig. 3, the solid lines are plotted by employing (6) while the markers are obtained by using Monte-Carlo simulations. We observe a good agreement between our framework and computer-based results thus, confirming the correctness of our framework. It is apparent that the larger the velocity of the train, the worse the OP. The explanation is simple as v increasing the estimated CSI is far from the actual one hence, decreasing the system performance. Additionally, Fig. 3 also unveils that the OP achieves the best performance when the train's position is close to the location of the APs. Although the best performance of the OP may climb up to 4×10^{-5} the worst performance is unacceptable were OP is equal to 1. As a consequence, optimal positions of both APs are necessary to minimize the outage event.

Fig. 4 shows the OP versus the x-coordinate of the train under Rayleigh and Nakagami-m distribution. It is evident that the OP performance under Nakagami-m fading is better than the OP under Rayleigh fading especially when the train is close to the locations of both APs. Particularly, we observe that the best OP under Nakagami-m fading is better than 1000-times compared to its counterpart.

Fig. 5 illustrates the ergodic capacity regarding the x-coordinate of the train under fixed deployment of APs. We observe a similar trend of the capacity and the outage probability with respect to the velocity that the larger the velocity, the smaller the capacity. Additionally, the mathematical framework in (7) absolutely with computer-based simulations results. Furthermore, Fig. 5 also confirms the necessity to optimally place the position of the APs to improve the system performance.

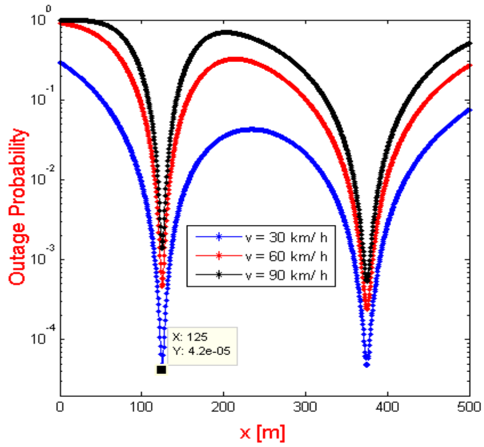

Fig. 3. Outage probability vs. the x-coordinate of the train with fixed deployment of APs with various value of velocity; solid lines from (6) and markers from Monte-Carlo simulations.

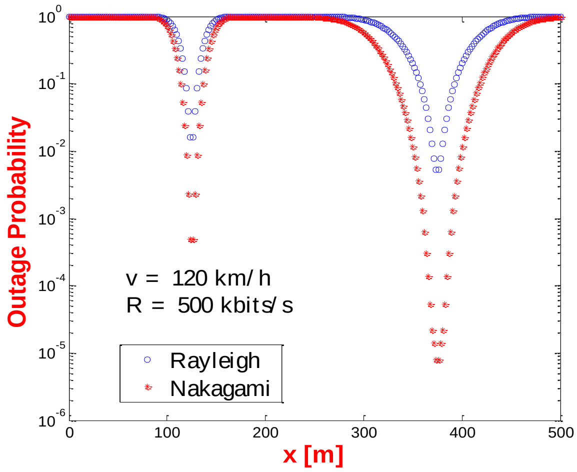

Fig. 4. Outage probability vs. the x-coordinate of the train with fixed deployment of APs with various fading distributions, i.e., Rayleigh, Nakagami-m with corresponding shape and scale parameters from APx, $x\in\{1, 2\}$, m={1.75, 2.25}and Ω={3.5, 4.5}; markers from Monte-Carlo simulations.

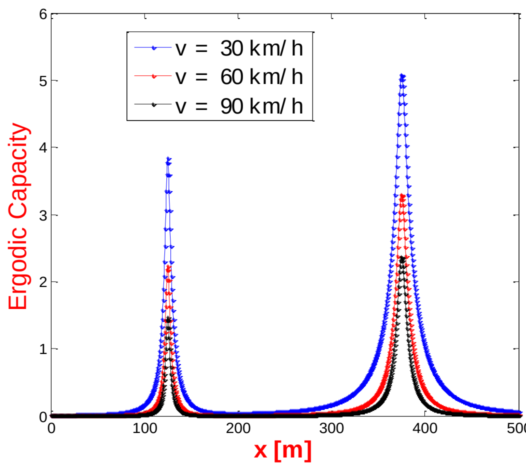

Fig. 5. Ergodic Capacity vs. the x-coordinate of the train with fixed deployment of APs with various value of velocity, i.e., v=30, 60, 90 km/h; solid lines from (7) and markers from Monte-Carlo simulations

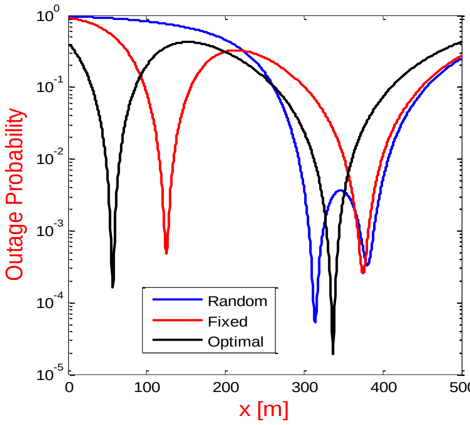

Fig. 6. Outage probability vs. the *x*-coordinate of the train with various deployments schemes.

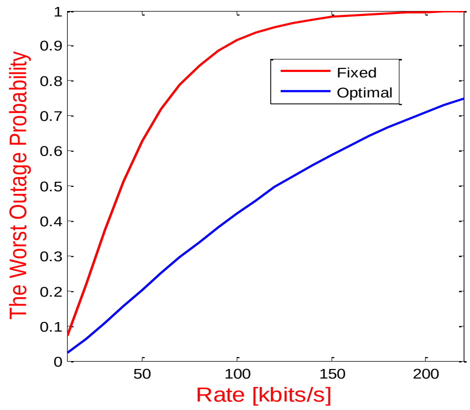

Fig. 7. The worst OP, i.e., $\max_{\tau}(\mathrm{OP}(\tau))$, vs. the achievable rate, i.e., *R*, under both "Optimal" and "Fixed" placement. The position of APs for case "Fixed" is the same as Fig. 3.

Fig. 6 depicts the outage performance versus the *x*-coordinator of the train under three different schemes, optimal, fixed and random deployment. The curve "Random" means the positions of AP1 and AP2 are uniformly deployed along the railway while the curve "Optimal" corresponds to the case both APs are optimally located. The coordination of AP1 and AP2 of curve "Fixed" are the same as Fig. 3. Again, we see that there always have two peaks for each curve which corresponds to the position of the APs. It is obvious that among three methods the "optimal" outperforms others in terms of both the worst and the best outage event. Let us investigate the worst scenario, we see that OP of "optimal" deployment is far better than the remained cases. Particularly, it is better than around two-fold compared to OP of both the "fixed" and "random" deployments.

Fig. 7 investigates the behavior of OP under the worst scenario, where the SNR_{e2e} is the lowest, versus the achievable rate under both "Optimal" and "Fixed" placement. When the target *R* is small, there is a small gap between two cases. However, when *R* is sufficiently large, we observe a significant gap. Specifically, the OP of the "Fixed" scheme starts equally to one when *R* approaches 200kbits/s while the OP under the "Optimal" deployment is still less than 1 even *R* equals to 220kbits/s. Furthermore, it is evident that increasing the achievable rate will obviously lead to raise the OP.

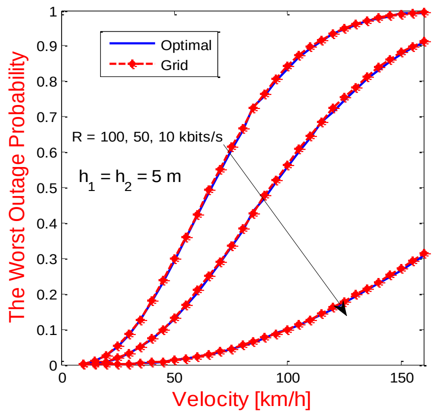

Fig. 8. The worst OP, i.e., $\max_{\tau}(\mathrm{OP}(\tau))$, vs. the velocity *v*, under both pattern search "Pattern" and grid (or exhaustive) search "Grid" with h_1=h_2=5m.

TABLE I. COMPARISON OF THE AVERAGE COMPUTING TIME (IN SECONDS) OVER V FOR OBTAINING THE OPTIMAL POSITIONS OF APS OF PATTERN SEARCH AND GRID SEARCH IN FIG. 6; *V*={10, 15, ⋯, 160}KM/H; THE STEP SIZE FOR GRID SEARCH IS 4 M.

	R=10	*R*=50	*R*=100
Pattern	0.1840	0.2303	0.2359
Grid	7.9704	8.7932	9.2361

Looking at Fig. 8, it is apparent that the proposed pattern search completely coincides with the grid search. Additionally, when the velocity goes up, the OP turns up. It can be explained that increasing *v* will evidently raise the path-loss; it, as a result, accelerates the outage probability. This figure also confirms our statements in Fig. 7 that the larger the target rate the sooner the OP approaching 1. This figure reveals an interesting fact that there is a similar behavior of the worst OP with respect to the velocity of the train and the target rate. Particularly, decrease either the velocity or the target rate will surely cut down the worst OP. From the system design prospective, it means that raising up the target rate in parallel with the increase of the train's velocity is harmful for the reliability aspect of the CBTC systems.

It is noted that this figure only optimizes two out of four variables, i.e., the *x*-coordinator of AP1 and AP2, x_1, x_2. Although both approaches provide the same performance the computation time is totally divergent. Table I compares the average time required to obtain the optimal solutions between two methods, pattern, and grid search in Fig. 8.

Observing Table I, we experience a huge gap between two methods in terms of the consuming time. More precisely, the required time based on grid search is bigger than its counterpart at least 38 times. Additionally, Table I shows the results which consider solely the *x*-coordinator of APs instead of both the horizontal and attitude of APs. Hence, pattern search obviously outperforms the exhaustive search in terms of the computation time.

Fig. 9 sketches the worst OP performance with respect to the path-loss exponent under the optimal placement scheme. More precisely, we observe that increasing η monotonically degrades the performance of the maximal outage probability. It means that when the transmission environment changes from less obstacles environment such as suburban, outskirts and countryside to dense obstacles ones, the behavior of the OP decreases significantly. Particularly, the OP dramatically increases from zero to one when η moves from 2.1 to 3.5 in case R =1kbits/s. Additionally, this figure also unveils that the higher the data rate the more outage event thus, deteriorating the considered CBTC systems. To be more specific, with R=50kbits/s, the system already stops working if η approximately 2.6. However, with R=1kbits/s, under the worst scenario, the outage event only appears less than 3%. Thus, to overcome the impact of the path-loss exponent, reducing the data-rate is an effective solution.

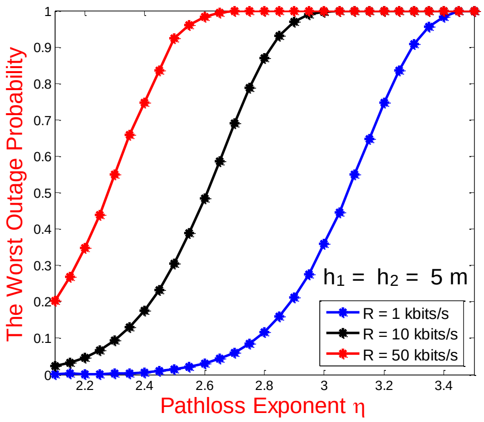

Fig. 9. The worst OP vs. the path-loss exponent, η.

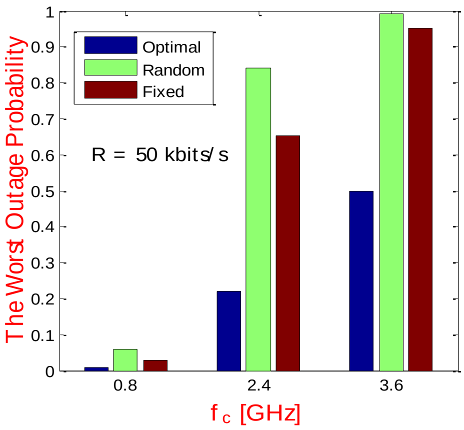

Fig. 10. The worst OP vs. the carrier frequency f_c.

Fig. 10 shows the impact of the carrier frequency on the performance of the worst outage probability. To be more specific, we consider three popular carrier frequency based on the standards of 802.11 family, namely, 802.11ah/b/g/n/ax/y [28]. It is expected that the performance of the optimal placement is superior to other placement schemes, i.e., the random and fixed deployment of the APs. Indeed, taking the 2.4 GHz as an example, the worst OP of the optimal location of the APs is far better than the others, i.e., four-fold and three-fold compared with the random and fixed deployment. Additionally, although moving up the carrier frequency will enhance the data-rate via broadening the transmission bandwidth, the OP is significant decrease due to the increase of the background noise.

VI. Conclusion

In this paper, we studied the performance of a CBTC system with two APs. Particularly, we derived the exact closed-form expression of the outage probability of the train under a practical scenario where the channel state information is imperfect owing to the mobility of the train. Based on the proposed mathematical framework, we minimized the worst case of the OP by optimally deploying the position of the APs. Our results proved that by optimal placement of the APs, the OP can be significantly improved. To further enhance the performance of the considered system, one may consider the help from the most advantage of wireless technology such as reconfigurable intelligent surface (RIS) technology [29], [30] or cell-free Massive MIMO system [31], [32] where the RIS panel acts as the relay to forwarding information from/to the train to the APs without consuming power thanks to its passive elements.

Conflict of Interest

The authors declare no conflict of interest.

Author Contributions

Do Viet Ha proposed the idea and wrote the manuscript. Tu Lam Thanh derived the mathematical framework and proofread the manuscript. Trinh Thi Huong was in charge of data curation and software. Trinh Van Chien conducted the numerical results and proofread the paper. All authors had approved the final version.

Acknowledgment

This research is funded by University of Transport and Communications (UTC) under grant number T2020-DT-005TĐ.

References

[1] J. G. Andrews, *et al*., "What will 5G be?" *IEEE J. Sel. Areas Commun.*, vol. 32, no. 6, pp. 1065-1082, June 2014.

[2] T. L. Thanh, A. Bradai, and Y. Pousset, "A new closed-form expression of the coverage probability for different QoS in LoRa networks," presented at the IEEE International Conference on Communications 2000 (ICC), Dublin, Ireland, 2020.

[3] R. D. Pascoe and T. N. Eichorn, "What is communication-based train control?" *IEEE Veh. Technol. Mag.*, vol. 4, no. 4, pp. 16-21, Dec. 2009.

[4] T. T. Lam and M. Di Renzo, "On the energy efficiency of heterogeneous cellular networks with renewable energy sources—A stochastic geometry framework," *IEEE Trans. Wireless Commun*., vol. 19, no. 10, pp. 6752-6770, Oct. 2020.

[5] T. L. Thanh, V. N. Q. Bao, and B. An, "On the performance of outage probability in underlay cognitive radio with imperfect CSI," in *Proc. International Conf. on Advanced Technologies for Communications*, Ho Chi Minh City, Vietnam, 2013, pp. 125-130.

[6] L. Zhu, F. R. Yu, B. Ning, and T. Tang, "Communication-based train control (CBTC) systems with cooperative relaying: Design and performance analysis," *IEEE Trans. Veh. Technol.*, vol. 63, no. 5, pp. 2162-2172, Jun. 2014.

[7] L. Zhu, F. R. Yu, B. Ning, and T. Tang, "Design and performance enhancements in communication-based train control systems with coordinated multipoint transmission and reception," *IEEE Trans. Intell. Transp. Syst.*, vol. 15, no. 3, pp. 1258-1272, June 2014.

[8] B. Bu, F. R. Yu, and T. Tang, "Performance improved methods

for communication-based train control systems with random packet drops," *IEEE Trans. Intell. Transp. Syst.*, vol. 15, no. 3, pp. 1179-1192, Jun. 2014.

[9] T. Tang, K. Dai, Y. Zhang, H. Zhao, and H. Jiang, "Field test results analysis in urban rail transit train ground communication systems of integrated service using LTE-M," in *Proc. of the IEEE 19th Inter. Conf. on Intell. Transp. Syst.*, Rio de Janeiro, Brazil, 2016, pp. 2017-2021.

[10] X. Wang, L. Liu, T. Tang, and W. Sun, "Enhancing communication-based train control systems through train-to-train communications," *IEEE Trans. Intell. Transp. Syst.*, vol. 20, no. 4, pp. 1544-1561, Apr. 2019.

[11] L. Wang, B. Ai, Y. Niu, X. Chen, and P. Hui, "Energy-efficient power control of train–ground mmwave communication for high-speed trains," *IEEE Trans. Veh. Technol.*, vol. 68, no. 8, pp. 7704-7714, Aug. 2019.

[12] H. Jiang, V. C. M. Leung, C. Gao, and T. Tang, "MIMO-assisted handoff scheme for communication-based train control systems," *IEEE Trans. Veh. Technol.*, vol. 64, no. 4, pp. 1578-1590, Apr. 2015.

[13] A. Fernández-Rodríguez, A. Fernández-Cardador, A. P. Cucala, M. Domínguez, and T. Gonsalves, "Design of robust and energy-efficient ATO speed profiles of metropolitan lines considering train load variations and delays," *IEEE Trans. Intell. Transp. Syst.*, vol. 16, no. 4, pp. 2061-2071, Aug. 2015.

[14] H. Wang, F. R. Yu, L. Zhu, T. Tang, and B. Ning, "A cognitive control approach to communication-based train control systems," *IEEE Trans. Intell. Transp. Syst.*, vol. 16, no. 4, pp. 1676-1689, Aug. 2015.

[15] X. Ling and K. L. Yeung, "Joint access point placement and channel assignment for 802.11 wireless LANs," *IEEE Trans. Wireless Commun.*, vol. 5, no. 10, pp. 2705–2711, Oct. 2006.

[16] A. Gondran, O. Baala, A. Caminada, and H. Mabed, "Joint optimization of access point placement and frequency assignment in WLAN," in *Proc. of the. 3rd IEEE/IFIP Int. Conf. Central Asia Internet*, Tashkent, Uzbekistan, Sep. 2007, pp. 1–5.

[17] X. Zhang, A. Ludwig, N. Sood, and C. D. Sarris, "Physics-based optimization of access point placement for train communication systems," *IEEE Trans. Intell. Transp. Syst.*, vol. 19, no. 9, pp. 3028-3038, Sept. 2018.

[18] T. Wen, C. Constantinou, L. Chen, Z. Tian, and C. Roberts, "Access point deployment optimization in CBTC data communication system," *IEEE Trans. Intell. Transp. Syst.*, vol. 19, no. 6, pp. 1985-1995, June 2018.

[19] T. L. Thanh, V. N. Q. Bao, and B. An, "On the performance of outage probability in underlay cognitive radio with imperfect CSI," in *Proc. of Int. Conf. Advanced Tech. for Commun.*, Ho Chi Minh City, Vietnam, 2013, pp. 125-130.

[20] I. S. Gradshteyn and I. M. Ryzhik, *Table of Integrals, Series, and Products*, 7thed. Elsevier Pte Ltd., 2007.

[21] T. L. Thanh, M. D. Renzo, and J. P. Coon, "MIMO cellular networks with simultaneous wireless information and power transfer," in *Proc. of 2016 IEEE 17th Inter. Work. Signal Processing Adv. in Wireless Commun.*, 2016, pp. 1-5.

[22] T. L. Thanh, M. Di Renzo and J. P. Coon, "System-level analysis of receiver diversity in SWIPT-enabled cellular networks," *J. of Commun. and Netw.*, vol. 18, no. 6, pp. 926-937, Dec. 2016.

[23] H. A. David and H. N. Nagaraja, *Order Statistics*, Wiley Series in Probability and Statistics, 2003.

[24] T. L. Thanh, V. N. Q. Bao and T. T. Duy, "Capacity analysis of multi-hop decode-and-forward over Rician fading channels," in *Proc. of 2014 International Conf. on Computing, Management and Telecommunications*, 2014, pp. 134-139.

[25] Wolfram Mathematica. [Online]. Available: https://functions.wolfram.com/06.34.02.0001.01

[26] R. Hooke and T. A. Jeeves, ""Direct search" solution of numerical and statistical problems," *J. of the ACM*, vol. 8, no. 2, pp. 212–229, Apr. 1961.

[27] B. Enrique; H. Alberto; P. José, "A direct search algorithm for global optimization," *MDPI Algorithms*, vol. 9, no. 2, 2016, Available: https://doi.org/10.3390/a9020040

[28] "WiFi Frequency Bands List," *Electronics Notes*, Retrieved 2021-06-03.

[29] T. V. Chien, L. T. Tu, S. Chatzinotas, and B. Ottersten, "Coverage probability and ergodic capacity of intelligent reflecting surface-enhanced communication systems," *IEEE Commun. Lett.*, vol. 25, no. 1, pp. 69-73, Jan. 2021.

[30] T. V. Chien, A. K. Papazafeiropoulos, L. T. Tu, R. Chopra, S. Chatzinotas, and B. Ottersten, "Outage probability analysis of IRS-assisted systems under spatially correlated channels," *IEEE Wireless Commun. Lett.*, May 2021.

[31] T. V. Chien, E. Björnson, and E. G. Larsson, "Optimal design of energy-efficient cell-free massive MIMO: Joint power allocation and load balancing," in *Proc. of ICASSP 2020*, Barcelona, Spain, 2020, pp. 5145-5149.

[32] T. V. Chien, E. Björnson, and Erik G. Larsson, "Joint power allocation and load balancing optimization for energy-efficient cell-free massive MIMO networks," *IEEE Trans. on Wireless Comm.*, vol. 19, no. 10, pp. 6798-6812, 2020.

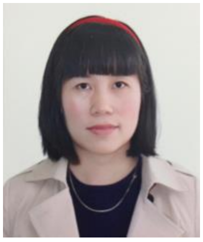

Do Viet Ha received the B.S, M.Sc., and Ph.D. degrees in electronic and telecommunication engineering from Hanoi University of Science and Technology (HUST), Hanoi, Vietnam, in 2001, 2007, and 2017, respectively. She is currently working with the Department of Telecommunication Engineering, University of Transport and Communications, Hanoi, Vietnam, as a lecturer. Her main areas of research interest are mobile channel modeling, especially underwater acoustic channels, underwater acoustic OFDM systems, and mobile-to-mobile communications.

Lam-Thanh Tu was born in 1986. He received his Ph.D. degree from the Laboratory of Signals and Systems of Paris-Saclay University, Paris, France. During the period 2015-2018, he was with French National Center for Scientific Research (CNRS), Paris, France, as an Early Stage Researcher of the European-funded project H2020 ETN-5Gwireless. Currently, he is a Research Fellow at the Institute Xlim, Poitiers University, Poitiers, France. His research interests include wireless communications and stochastic geometry.

Trinh Thi Huong received bachelor and master degrees in electronics and telecommunications from University of Transport and Communications, Hanoi, Vietnam in 2003 and 2006, respectively. She completed her Ph.D. degree in 2018 in telecommunication engineering from Hanoi University of Science and Technology (HUST), Hanoi, Vietnam. She is a lecturer at Faculty of Electrical and Electronic Engineering, University of Transport and Communications, Hanoi, Vietnam. Her research interests include space-time signal processing, advanced wireless communication and localisation systems for high speed rail.

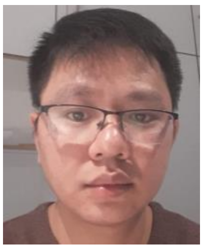

Trinh Van Chien received the B.S. degree in Electronics and Telecommunications from Hanoi University of Science and Technology (HUST), Vietnam, in2012. He then received the M.S. degree in Electrical and Computer Engineering from Sungkyunkwan University (SKKU), Korea, in 2014 and the Ph.D. degree in Communication Systems from Linkoping University (LiU), Sweden, in 2020. His interest lies in convex optimization problems for wireless communications and image & video processing. He was an IEEE wireless communications letters exemplary reviewer for 2016 and 2017. He also received the award of scientific excellence in the first year of the 5Gwireless project funded by European Union Horizon's2020.